

# X-ray and neutron powder diffraction study of the double perovskites $\text{Ba}_2\text{LnSbO}_6$ ( $\text{Ln} = \text{La}, \text{Pr}, \text{Nd}$ and $\text{Sm}$ )

W.T. Fu\*, D.J.W. IJdo

*Leiden Institute of Chemistry, Gorlaeus Laboratories, Leiden University, P.O. Box 9502, 2300 RA Leiden, The Netherlands*

Received 10 March 2005; received in revised form 10 May 2005; accepted 20 May 2005

## Abstract

The crystal structures of  $\text{Ba}_2\text{LnSbO}_6$  ( $\text{Ln} = \text{La}, \text{Pr}, \text{Nd}$  and  $\text{Sm}$ ) at room temperature have been investigated by profile analysis of the Rietveld method using either combined X-ray and neutron powder diffraction data or X-ray powder diffraction data. It has been shown that the structure of  $\text{Ba}_2\text{LnSbO}_6$  with  $\text{Ln} = \text{La}, \text{Pr}$  and  $\text{Nd}$  are neither monoclinic nor cubic as were previously reported. They are rhombohedral with the space group  $R\bar{3}$ . The distortion from cubic symmetry is due to the rotation of the  $\text{LnO}_6/\text{SbO}_6$  octahedra about the primitive cubic  $[111]_p$ -axis. On the other hand, the structure of  $\text{Ba}_2\text{SmSbO}_6$  is found to be cubic. All compounds contain an ordered arrangement of  $\text{LnO}_6$  and  $\text{SbO}_6$  octahedra.

© 2005 Elsevier Inc. All rights reserved.

**Keywords:** Perovskites; X-ray powder diffraction; Neutron powder diffraction; Crystal structure

## 1. Introduction

Ternary compounds of the formula  $\text{ABX}_3$  often crystallise in the perovskite structure. Depending on the tolerance factor,  $t = (r_A + r_B)/\sqrt{2}(r_B + r_X)$ , where  $r_A$ ,  $r_B$  and  $r_X$  are the constituent ionic radii, a perovskite may adopt either the simple cubic structure ( $t \approx 1$ ), space group  $Pm\bar{3}m$ , or a distorted one ( $t > 1$  or  $t < 1$ ), with lower symmetry. For the majority of perovskites known so far, the distortions from the ideally cubic structure were found to be due to the tilting of the  $\text{BX}_6$  octahedra. Glazer [1,2] classified the tilting patterns in terms of independent tilts of the rigid octahedra around the pseudo-cubic axes, and obtained 23 possible tilt systems with the corresponding space groups. Woodward [3,4] re-examined the Glazer's tilt systems and found that in six of the tilt systems it is not possible to maintain perfectly rigid octahedra; small distortions of octahedra should occur. Recently, Howard and Stokes [5] undertook a group-theoretical analysis of the

Glazer's tilt system and derived 15 possible space groups.

The double perovskites,  $\text{A}_2\text{BB}'\text{X}_6$ , are derived from the  $\text{ABX}_3$  perovskites when half of the octahedrally coordinated  $B$ -cations are replaced by the suitable  $B'$ -cations. If an ordered arrangement between  $B$  and  $B'$  occurs, the symmetry and the size are changed. One may define the tolerance factor for  $\text{A}_2\text{BB}'\text{X}_6$  double perovskites as  $t = (r_A + r_B)/\sqrt{2}(\bar{r}_{(B,B')} + r_X)$ , where  $\bar{r}_{(B,B')}$  is the averaged ionic radii of the  $B$  and  $B'$ -cation. The ideal double perovskite has the cubic symmetry ( $t \approx 1$ ), space group  $Fm\bar{3}m$ , with a unit cell edge double that of the cubic  $\text{ABX}_3$  aristotype. If there is mismatch between the  $A$ - $X$  and the averaged  $(B,B')$ - $X$  bond lengths, i.e.  $t > 1$  or  $t < 1$ , the structure of the double perovskites distorts from cubic symmetry. Just like the normal perovskites, the most commonly occurred distortions in  $\text{A}_2\text{BB}'\text{X}_6$  are due to the tilting of the  $\text{BX}_6/B'\text{X}_6$  octahedra. Woodward [3], based on the Glazer's description of the tilt systems, has considered the cation ordering and octahedral tilting occurring simultaneously and derived 13 possible space groups for double perovskites. Howard et al. [6] identified, using the group-theoretical analysis, 12 space

\*Corresponding author. fax: +31 71 5274537.

E-mail address: [w.fu@chem.leidenuniv.nl](mailto:w.fu@chem.leidenuniv.nl) (W.T. Fu).

groups under the same conditions of the octahedral tilting and the cation ordering.

The compounds of the formula  $\text{Ba}_2\text{LnSbO}_6$  ( $\text{Ln}$  = lanthanides) have long been known since Blasse first reported  $\text{Ba}_2\text{GdSbO}_6$  to be double cubic with 1:1 ordering of Gd(III) and Sb(V) ions [7]. Later on, the other compounds with heavier lanthanides were proved, by X-ray powder diffraction, to be double cubic [8], but the coordinates of the oxygen atoms were not given. Alonso et al. [9] have determined, using neutron powder diffraction data, the structure of  $\text{Ba}_2\text{LnSbO}_6$  in the case of  $\text{Ln} = \text{Ho}$  and Y, and confirmed the cubic space group  $Fm\bar{3}m$ . For compounds with lighter lanthanides, the crystal structures seem to be less well characterised. Wittmann et al. [10] reported a monoclinic cell for  $\text{Ba}_2\text{LnSbO}_6$  with  $\text{Ln} = \text{La}$ , Pr and Nd, and a primitive cubic cell for  $\text{Ba}_2\text{SmSbO}_6$ , respectively. However, Kurian et al [11] prepared  $\text{Ba}_2\text{LnSbO}_6$  ( $\text{Ln} = \text{Pr}$ , Sm and Gd) as substrates for high- $T_c$  superconducting  $\text{Ba}_2\text{YCu}_3\text{O}_{7-\delta}$  and described them to be double cubic perovskites. But from their reported X-ray powder diffraction pattern of  $\text{Ba}_2\text{PrSbO}_6$ , the splitting of diffraction lines is clearly visible suggesting that its symmetry should be lower than cubic. We, therefore, carried out a structural study on the compounds  $\text{Ba}_2\text{LnSbO}_6$  ( $\text{Ln} = \text{La}$ , Pr, Nd and Sm) and report their correct space groups and crystal structures in this paper.

## 2. Experimental

Samples of  $\text{Ba}_2\text{LnSbO}_6$  ( $\text{Ln} = \text{La}$ , Pr, Nd, and Sm) were prepared from  $\text{BaCO}_3$ ,  $\text{La}_2\text{O}_3$ ,  $\text{Pr}_6\text{O}_{11}$ ,  $\text{Nd}_2\text{O}_3$ ,  $\text{Sm}_2\text{O}_3$ , and  $\text{Sb}_2\text{O}_3$  in alumina crucibles using the standard solid-state reaction in air. The hygroscopic  $\text{La}_2\text{O}_3$  and  $\text{Nd}_2\text{O}_3$  were preheated at  $1000^\circ\text{C}$  for several hours before use. Due to the low melting point of  $\text{Sb}_2\text{O}_3$ , the mixtures were first heated at  $800^\circ\text{C}$  overnight. The resultant powders were then sintered with a temperature step of  $100^\circ\text{C}$  and 20 h at each step with regrinding. The final sintering temperature was  $1300^\circ\text{C}$ . The samples were furnace cooled to room temperature.

X-ray diffraction patterns were collected with a Philips PW1050 diffractometer using  $\text{Cu-K}\alpha$  radiation in steps of  $0.02^\circ$  ( $2\theta$ ) and 12 s counting time in the range of  $10^\circ < 2\theta < 116^\circ$ . The neutron powder diffraction data were collected at room temperature for  $\text{Ba}_2\text{LnSbO}_6$  ( $\sim 20$  g),  $\text{Ln} = \text{La}$  and Pr, on the powder diffractometer of the High-Flux Reactor of NRG in Petten, with the neutron wavelength of  $1.4258 \text{ \AA}$  and in steps of  $0.05^\circ$  ( $2\theta$ ). Vanadium can was used as sample holder. For neutron powder diffraction data, the absorption corrections were applied according to Weber [12].

Model refinement was performed by the Rietveld method using the Rietica computer program [13]. No anomalous scattering corrections were applied. A

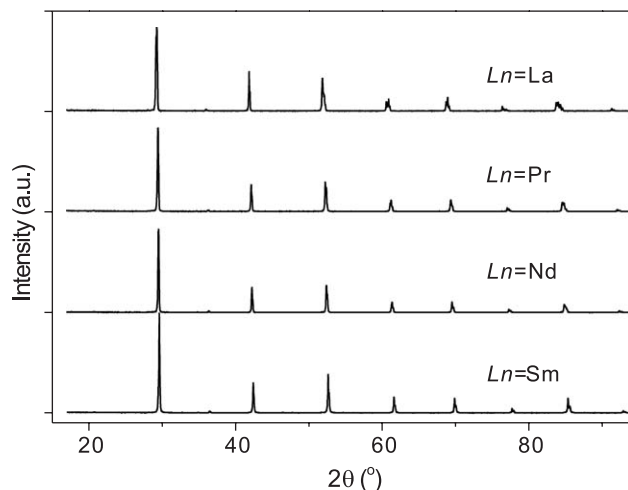


Fig. 1. X-ray powder diffraction patterns of  $\text{Ba}_2\text{LnSbO}_6$  ( $\text{Ln} = \text{La}$ , Pr, Nd and Sm).

polynomial function with six parameters was used to fit the background. The profiles have been fitted using a Pseudo-Voigt function with peak asymmetric correction. The neutron scattering lengths used in the calculation are:  $b_{(\text{Ba})} = 5.06$ ,  $b_{(\text{La})} = 8.24$ ,  $b_{(\text{Pr})} = 4.58$ ,  $b_{(\text{Sb})} = 5.57$  and  $b_{(\text{O})} = 5.803 \text{ fm}$ .

## 3. Results

X-ray diffraction patterns of  $\text{Ba}_2\text{LnSbO}_6$  at room temperature are shown in Fig. 1. They all show strong lines characteristic of a primitive cubic cell. However, many of the diffraction lines are visibly split for  $\text{Ln} = \text{La}$ , Pr and Nd, indicating that the symmetry is lower than cubic (see also Fig. 2). In addition, a few very weak additional lines, indicative of the presence of a supercell in these compounds, are also visible. Due to quite small difference in the scattering power to X-ray between  $\text{Ln}$  and Sb atoms, all superlattice diffraction lines due to their ordering are of low intensity. However, the cation ordering is clearly revealed by neutron powder diffraction data (Fig. 3). To identify the possible space groups for  $\text{Ba}_2\text{LnSbO}_6$ , we have examined both the occurrence of the superlattice diffraction lines and the splitting of diffraction peaks corresponding to the basic cubic perovskite cell. As can be seen from both X-ray (Fig. 1) and neutron (Fig. 3) powder diffraction patterns, all observed superlattice diffraction lines are indexed in terms of a double cubic cell all with odd indices. This suggests that only out-of-phase tilting of the octahedra, if it exists, is possible. Considering further that the octahedral tilting occurs around one of the principle axes of the basic cubic perovskite cell,<sup>1</sup>

<sup>1</sup>We found, from our X-ray diffraction data, no evidence to suggest the triclinic symmetry, such as  $F\bar{1}$  (tilt system  $(a^-b^-c^-)$ ) or  $I\bar{1}$  (tilt system  $(a^0b^-c^-)$ ), for  $\text{Ba}_2\text{LnSbO}_6$ .

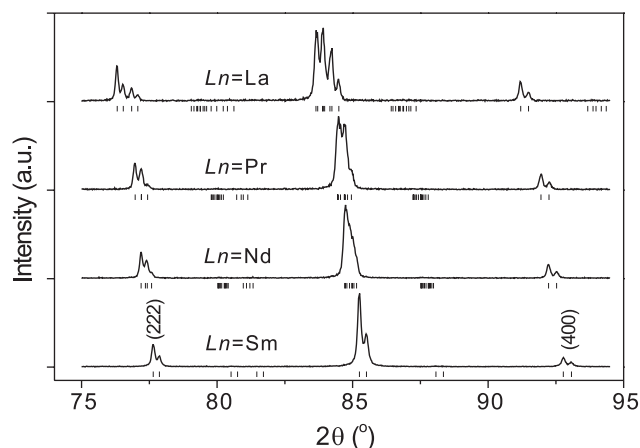


Fig. 2. An enlarged section of the diffraction patterns of  $\text{Ba}_2\text{LnSbO}_6$  showing the basic (222) and (400) reflections. The tick marks below are the calculated positions of the allowed Bragg's reflections using the refined lattice parameters in the space groups  $R\bar{3}$  ( $\text{Ln} = \text{La}, \text{Pr}, \text{Nd}$ ) and  $Fm\bar{3}m$  ( $\text{Ln} = \text{Sm}$ ), respectively. Note that the basic (222) reflection splits in the rhombohedral cell in the (400) and (444) reflections.

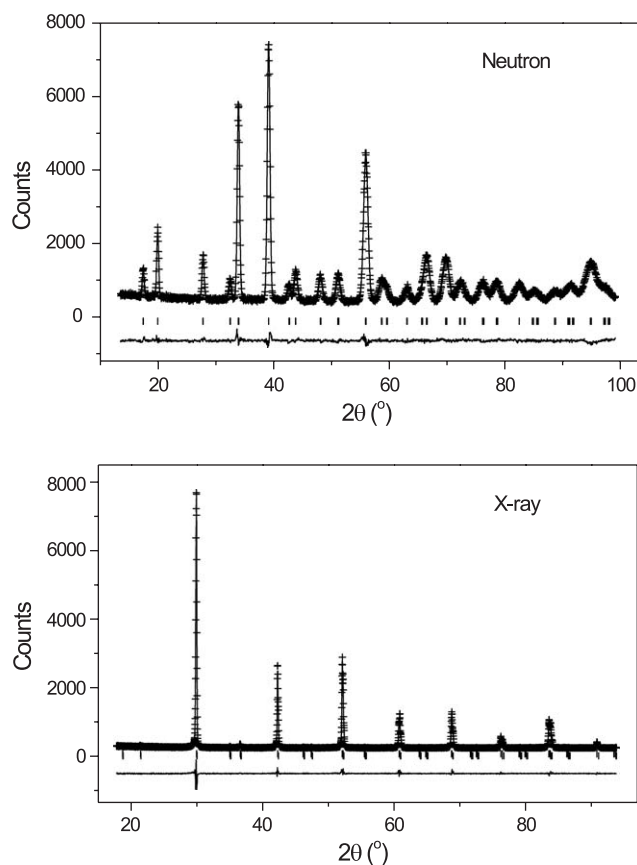


Fig. 3. Observed (crosses) and calculated (full line) profiles of both neutron and X-ray powder diffraction for  $\text{Ba}_2\text{PrSbO}_6$ . Tick marks below the profiles indicate the positions of the Bragg reflections. A difference curve (observed-calculated) is shown at the bottom of the plots.

i.e.  $[001]_p$ ,  $[110]_p$  and  $[111]_p$ -axis, the structure of  $\text{Ba}_2\text{LnSbO}_6$  would have one of the following possible space groups:  $I4/m$  ( $a^0a^0c^-$ ),  $I2/m$  ( $a^0b^-b^-$ ) and  $R\bar{3}$  ( $a^-a^-a^-$ ) including the one without tilting,  $Fm\bar{3}m$  ( $a^0a^0a^0$ ) [3,6]. Close inspection of the main peak splitting has ruled out both  $I4/m$  and  $I2/m$  as possible space groups (Fig. 2). For example, the basic (400) would split into two in both  $I4/m$  and  $I2/m$ , but it clearly remains as one single peak; only splitting due to  $K\alpha_1$  and  $K\alpha_2$  radiations is resolved. Further examination of the basic (222) reflection showed a structural change from rhombohedral to cubic through  $\text{La} \rightarrow \text{Sm}$ . For instance, the basic (222) diffraction line of  $\text{Ba}_2\text{LaSbO}_6$  splits into two, which are indexed as (400) and (444), as is expected for the space group  $R\bar{3}$ . The degree of splitting becomes progressively smaller for  $\text{Ln} = \text{Pr}$  and  $\text{Nd}$ , and the splitting is no more visible for  $\text{Ln} = \text{Sm}$ . In fact, all diffraction lines of  $\text{Ba}_2\text{SmSbO}_6$  showed no splitting except that being due to  $K\alpha_1$  and  $K\alpha_2$  radiations. Consequently, the likely space groups of  $\text{Ba}_2\text{LnSbO}_6$  are  $R\bar{3}$  for  $\text{Ln} = \text{La}, \text{Pr}$  and  $\text{Nd}$  and  $Fm\bar{3}m$  for  $\text{Ln} = \text{Sm}$ , respectively.

The Rietveld refinements were carried out in the space groups  $R\bar{3}$  and  $Fm\bar{3}m$  to model the structures of  $\text{Ba}_2\text{LnSbO}_6$ . Considering that the neutron diffraction is more sensitive to the octahedral tilting and the cation ordering and that the X-ray diffraction provides more information on the symmetry of the lattice and the positions of the heavier cations, the structure of  $\text{Ba}_2\text{LnSbO}_6$  with  $\text{Ln} = \text{La}$  and  $\text{Pr}$  were refined from the combined neutron and X-ray powder diffraction data [14]. For compounds with  $\text{Ln} = \text{Nd}$  and  $\text{Sm}$ , no neutron diffraction data were available; only X-ray powder diffraction data were used in the calculations. In all cases, Rietveld refinements yielded satisfactory results. The refined structural and thermal parameters are summarised in Table 1. Table 2 lists some selected inter atomic distances. The plots of the observed and calculated profiles of both neutron and X-ray diffraction of  $\text{Ba}_2\text{PrSbO}_6$  are shown in Fig. 3.

#### 4. Discussion

The crystal structures of  $\text{Ba}_2\text{LnSbO}_6$  ( $\text{Ln} = \text{La}, \text{Pr}, \text{Nd}$  and  $\text{Sm}$ ) are easily derived from the simple cubic aristotype by ordering the octahedral cations in a 1:1 ordering scheme (Fig. 4). In  $\text{Ba}_2\text{LnSbO}_6$  ( $\text{Ln} = \text{La}, \text{Pr}, \text{Nd}$ ), the  $\text{LnO}_6$  and  $\text{SbO}_6$  octahedra are tilted around the three-fold  $[111]_p$ -axis, resulting in rhombohedral symmetry. In  $\text{Ba}_2\text{SmSbO}_6$ , no octahedral tilting is observed. Such a structural change is expected given the systematic change of the match between the  $\text{Ba}-\text{O}$  and the averaged  $(\text{Ln}, \text{Sb})-\text{O}$  ( $\text{Ln} = \text{lanthanide}$ ) bond lengths. The tolerance factor of  $\text{Ba}_2\text{LaSbO}_6$  is  $t = 0.96$ , indicating that the  $\text{Ba}$  atoms are somewhat smaller to fit in the cavity

Table 1

Refined atomic positions and thermal parameters of  $\text{Ba}_2\text{LnSbO}_6$  ( $\text{Ln} = \text{La}, \text{Pr}, \text{Nd}$  and  $\text{Sm}$ ) in the space groups  $R\bar{3}$  and  $Fm\bar{3}m$ 

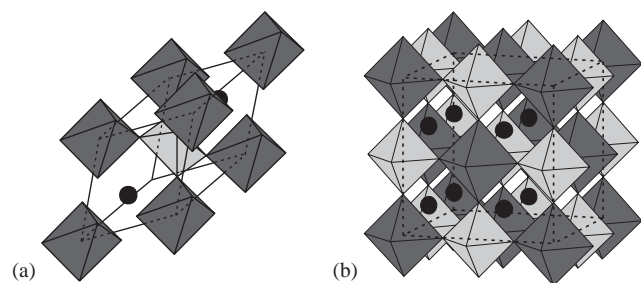
$\text{Ba}_2\text{LaSbO}_6$ ( $R\bar{3}$ )		$\text{Ba}_2\text{PrSbO}_6$ ( $R\bar{3}$ )		$\text{Ba}_2\text{NdSbO}_6$ ( $R\bar{3}$ )		$\text{Ba}_2\text{SmSbO}_6$ ( $Fm\bar{3}m$ )	
$a$ (Å)	6.0825(1)	$a$ (Å)	6.0549(1)	$a$ (Å)	6.04003(9)	$a$ (Å)	8.50908(8)
$\alpha$ (°)	60.292(1)	$\alpha$ (°)	60.124(2)	$\alpha$ (°)	60.086(1)		
Ba	$2c$ ( $x, x, x$ )	Ba	$2c$ ( $x, x, x$ )	Ba	$2c$ ( $x, x, x$ )	Ba	$8c$ (0.25,0.25,0.25)
$x$	0.2513(2)	$x$	0.2509(3)	$x$	0.2501(4)	$B(\text{Å})^2$	0.56(2)
$B(\text{Å})^2$	0.38(2)	$B(\text{Å})^2$	0.26(2)	$B(\text{Å})^2$	0.47(2)	Sm	$4a$ (0,0,0)
La	$1a$ (0,0,0)	Pr	$1a$ (0,0,0)	Nd	$1a$ (0,0,0)	Sm	$4a$ (0,0,0)
$B(\text{Å})^2$	0.02(4)	$B(\text{Å})^2$	0.17(7)	$B(\text{Å})^2$	0.15(2)	$B(\text{Å})^2$	0.54(7)
Sb	$1b$ (0.5,0.5,0.5)	Sb	$1b$ (0.5,0.5,0.5)	Sb	$1b$ (0.5,0.5,0.5)	Sb	$4b$ (0.5,0.5,0.5)
$B(\text{Å})^2$	0.15(5)	$B(\text{Å})^2$	0.01(1)	$B(\text{Å})^2$	0.15(2)	$B(\text{Å})^2$	0.13(8)
O	$6f$ ( $x, y, z$ )	O	$6f$ ( $x, y, z$ )	O	$6f$ ( $x, y, z$ )	O	$24e$ ( $x,0,0$ )
$x$	-0.2771(7)	$x$	-0.2860(6)	$x$	-0.279(4)	$x$	0.258(2)
$y$	0.2307(2)	$y$	0.2393(4)	$y$	0.240(5)	$B(\text{Å})^2$	1.1(1)
$z$	0.3097(2)	$z$	0.2925(7)	$z$	0.276(4)		
$B(\text{Å})^2$	0.96(2)	$B(\text{Å})^2$	0.94(2)	$B(\text{Å})^2$	1.0(1)		
$R_{\text{wp}} = 4.02\%^a$ (17.90%) <sup>b</sup>		$R_{\text{wp}} = 4.16\%^a$ (16.96%) <sup>b</sup>		$R_{\text{wp}} = 16.42\%^b$		$R_{\text{wp}} = 16.53\%^b$	
$R_{\text{p}} = 2.82\%^a$ (11.72%) <sup>b</sup>		$R_{\text{p}} = 3.29\%^a$ (10.88%) <sup>b</sup>		$R_{\text{p}} = 10.45\%^b$		$R_{\text{p}} = 10.31\%^b$	
$R_{\text{B}} = 1.28\%^a$ (3.24%) <sup>b</sup>		$R_{\text{B}} = 1.61\%^a$ (6.30%) <sup>b</sup>		$R_{\text{B}} = 2.54\%^b$		$R_{\text{B}} = 4.24\%^b$	
$\chi^2 = 3.62^a$ (2.23) <sup>b</sup>		$\chi^2 = 1.96^a$ (2.14) <sup>b</sup>		$\chi^2 = 2.70$		$\chi^2 = 3.06$	

<sup>a</sup> $R$ -factor of neutron diffraction data.<sup>b</sup> $R$ -factor of X-ray diffraction data.

Table 2

Selected interatomic distances (Å) and the tilting angle of the octahedra (°)

	$\text{Ba}_2\text{LaSbO}_6$	$\text{Ba}_2\text{PrSbO}_6$	$\text{Ba}_2\text{NdSbO}_6$	$\text{Ba}_2\text{SmSbO}_6$
Ln–O	2.342(1) 6 ×	2.290(3) 6 ×	2.22(3) 6 ×	2.20(2) 6 ×
Sb–O	1.996(1) 6 ×	2.015(4) 6 ×	2.07(4) 6 ×	2.06(2) 6 ×
Ba–O	2.819(1) 3 ×	2.877(2) 3 ×	2.90(4) 3 ×	3.0092(5) 12 ×
	2.996(5) 3 ×	2.902(6) 3 ×	2.92(1) 3 ×	
	3.113(5) 3 ×	3.167(6) 3 ×	3.14(1) 3 ×	
	3.342(1) 3 ×	3.200(2) 3 ×	3.15(4) 3 ×	
$\varphi$ (°)	7.8	5.3	3.6	0

Fig. 4. Schematic representation of the crystal structures of rhombohedral  $\text{Ba}_2\text{LnSbO}_6$  ( $\text{Ln} = \text{La}, \text{Pr},$  and  $\text{Nd}$ ) (a) and cubic  $\text{Ba}_2\text{SmSbO}_6$  (b), showing the  $\text{LnO}_6$  (dark shaded) and  $\text{SbO}_6$  (light shaded) octahedra and the Ba atoms (black).

formed by the  $\text{LaO}_6$  and  $\text{SbO}_6$  octahedra. The tilting of octahedra reduces the size of cavity by reducing some of the Ba–O distances. As the ionic radius of the lanthanide diminishes from La to Nd, the mismatch between Ba–O

and the averaged (Ln,Sb)–O bond-lengths decreases. This can also be seen from the magnitude of the averaged tilting angle ( $\varphi$ ) calculated from the coordinates of the oxygen atom using the formula [15]:  $\tan(\varphi) = \sqrt{3}(z - y)$  (rad). For  $\text{Ln} = \text{La}, \text{Pr}$  and  $\text{Nd}$ , the tilting angles are  $7.8^\circ, 5.3^\circ$  and  $3.6^\circ$ , respectively, being in agreement with the increasing of the tolerance factors, 0.96, 0.97 and 0.971, respectively. It is also noticed that several known ordered perovskites that do adopt the rhombohedral space group  $R\bar{3}$ , e.g.  $\text{Ba}_2\text{BiSbO}_6$  ( $t = 0.961$ ) [16],  $\text{Ba}_2\text{YbBiO}_6$  ( $t = 0.961$ ) [17],  $\text{Ba}_2\text{LaIrO}_6$  ( $t = 0.967$ ) [18],  $\text{Ba}_2\text{BiTaO}_6$  ( $t = 0.952$ ) [19], all have the comparable values of the tolerance factor. With further decreasing the size of lanthanide, e.g.  $\text{Ln} = \text{Sm}$ , no bond length mismatch apparently exists, and the ordered perovskites have the double cubic structure as were also confirmed previously for  $\text{Ln} = \text{Gd}$  [7], Ho and Y [9].

Our results are in agreement with the earlier finding of Wittmann et al. [10] that the compounds with  $\text{Ln} = \text{La}, \text{Pr},$  and  $\text{Nd}$  are non-cubic, but differ with their description as monoclinic. As was mentioned above, octahedral tilting around the twofold  $[110]_{\text{p}}$ -axis would result in monoclinic symmetry with the space group  $I2/m$ . In this space group, however, the basic ( $h00$ )-type would split into two, which is clearly not the case. On the other hand, we confirmed the cubic structure of  $\text{Ba}_2\text{SmSbO}_6$  as was reported by Kurian et al. [11], but their description of  $\text{Ba}_2\text{PrSbO}_6$  being also double cubic is now wrong.

It is interesting to note that the calculated tolerance factor of  $\text{Ba}_2\text{SmSbO}_6$  ( $t = 0.977$ ) deviates quite a bit from unity. It has nevertheless the cubic symmetry

without any octahedral tilt. As compared to the cubic  $ABX_3$  aristotype, in which the only variable parameter is the cell length, the structure of double cubic  $A_2BB'X_6$  has an additionally adjustable parameter, i.e. the position of  $X$ -anion in-between the  $B$  and  $B'$  cations, so that the relative sizes of  $B$  and  $B'$  could be adjusted. It may, therefore, release, at certain extent, the mismatch between the  $A$ – $X$  bond length and the averaged  $(B, B')$ – $X$  bond length in double perovskite structure. In fact, in  $Ba_2LnSbO_6$  the  $Ln$ –O bond lengths are all smaller (Table 2) than the sum of the corresponding ionic radii [20]. For example, the bond lengths of La–O and Pr–O are found to be 2.342 Å and 2.290 Å as were compared to the calculated values of 2.432 and 2.390, respectively. On the other hand, the observed Sb–O bond lengths are quite compatible with that from the sum of ionic radii (2.00 Å). The same feature has also been found in the cubic perovskites  $Ba_2HoSbO_6$  and  $Ba_2YSbO_6$  [9] as well as in the rhombohedral  $Ba_2BiSbO_6$  [16]. Given that  $Ba_2SmSbO_6$  ( $t = 0.977$ ) is a double cubic perovskite, it is expected that other  $Ba_2B(III)B'(V)O_6$ -type perovskites with comparable values of the tolerance factor should also adopt the double cubic structure. Indeed, our recent investigations on  $Ba_2NdIrO_6$  ( $t = 0.978$ ),  $Ba_2PrRuO_6$  ( $t = 0.977$ ),  $Ba_2NdRuO_6$  ( $t = 0.979$ ),  $Ba_2NdIrO_6$  ( $t = 0.978$ ) and  $Ba_2HoNbO_6$  ( $t = 0.981$ ) showed that they all have cubic symmetry at room temperature. The detailed results on these perovskites will be published elsewhere. Finally, we want to mention that the compound  $Ba_2LnSbO_6$  with  $Ln = Ce$  does not exist. In this case, Ce is tetravalent leading to a cation-deficient perovskite of the formula  $Ba_2Ce_{0.75}SbO_6$ , space group  $I4/mmm$  [21], with complete ordering of Ce, Sb and vacancies.

In conclusion, we have studied the structures of the double perovskites  $Ba_2LnSbO_6$  ( $Ln = La, Pr, Nd$  and  $Sm$ ) at room temperature, using either the combined X-ray and neutron powder diffraction or X-ray powder diffraction techniques alone. They all contain the ordered arrangement of  $LnO_6$  and  $SbO_6$  octahedra but with different symmetries. In  $Ba_2LnSbO_6$  whose tolerance factor deviates largely from the unity, the octahedra are tilted around the primitive  $[111]_p$ -axis of the cubic aristotype, resulting in the space group  $R\bar{3}$ . Examples are  $Ln = La, Pr,$  and  $Nd$ . For smaller lanthanides, i.e. from  $Sm$  downwards, no octahedral

tilting occurs, and  $Ba_2LnSbO_6$  have the simple double cubic structure with the space group  $Fm\bar{3}m$ . For a number of  $Ba_2B(III)B'(V)O_6$ -type perovskites, it seems that the double cubic structure exists with the tolerance factor ( $t$ ) of about above 0.98.

## Acknowledgments

The authors are indebted to Mr. A. Bontenbal of NRG in Petten for the collection of the powder neutron diffraction data and to Dr. R.A.G. de Graaff for valuable discussions.

## References

- [1] A.M. Gazer, Acta Crystallogr. B 28 (1972) 3384.
- [2] A.M. Gazer, Acta Crystallogr. A 31 (1975) 756.
- [3] P.M. Woodward, Acta Crystallogr. B 53 (1997) 32.
- [4] P.M. Woodward, Acta Crystallogr. B 53 (1997) 44.
- [5] C.J. Howard, H.T. Stokes, Acta Crystallogr. B 54 (1998) 782.
- [6] C.J. Howard, B.J. Kennedy, P.M. Woodward, Acta Crystallogr. B 59 (2003) 463.
- [7] G. Blasse, J. Inorg. Nucl. Chem. 27 (1965) 993.
- [8] P. Garcia-Casado, A. Mendiola, I. Rasines, Z. Anorg. Allg. Chem. 510 (1984) 194.
- [9] J.A. Alonso, C. Cascales, P. Garcia-Casado, I. Rasines, J. Solid State Chem. 128 (1997) 247.
- [10] U. von Wittmann, G. Rauser, S. Kemmler-Sack, Z. Anorg. Allg. Chem. 482 (1981) 143.
- [11] J. Kurian, J. Koshi, P.R.S. Wariar, Y.P. Yadava, A.D. Damodaran, J. Solid State Chem. 116 (1995) 193.
- [12] K. Weber, Acta Crystallogr. 23 (1967) 720.
- [13] C.J. Howard, B.A. Hunter, A computer program for Rietveld analysis of X-ray and neutron powder diffraction patterns, Lucas Height Research Laboratories, 1998.
- [14] R.B. Von Dreele, in: R.A. Young (Ed.), The Rietveld Method, Oxford University Press, Oxford, 1993 (Chapter 12).
- [15] S. Pei, J.D. Jorgensen, B. Dabrowski, D.G. Hinks, D.R. Richards, A.W. Mitchell, J.M. Newsam, S.K. Sinha, D. Vaknin, A.J. Jacobson, Phys. Rev. B 41 (1990) 4126.
- [16] W.T. Fu, Solid State Commun. 116 (2000) 461.
- [17] W.T.A. Harrison, K.P. Reis, A.J. Jacobson, L.F. Schneemeyer, J.V. Waszczak, Chem. Mater. 7 (1995) 2161.
- [18] W.T. Fu, D.J.W. IJdo, J. Alloys Compd. 394 (2005) L5–L8.
- [19] K.S. Wallwork, B.J. Kennedy, Q. Zhou, Y. Lee, T. Vogt, J. Solid State Chem. 178 (2005) 207.
- [20] R.D. Shannon, Acta Cryst. A 32 (1976) 751.
- [21] D.J.W. IJdo, R.B. Helmholtz, Acta Cryst. C 49 (1993) 652.